NOSTRADAMVS, LLC

# MIMO SYSTEMS: DIVERSITY, BEAMFORMING, AND SPATIAL MULTIPLEXING

**WHITE PAPER**

v1.0
May 2023
Nostradamvs, LLC

## SUMMARY

This paper explores the powerful combination of MIMO diversity, beamforming, and spatial multiplexing techniques for revolutionizing wireless communication. Using their individual strengths and synergistic effects, we reveal how these technologies can significantly enhance signal quality, mitigate interference, and increase network capacity. Discover the transformational potential of this triad in next-generation wireless systems.

www.nostradamvsllc.com

# Table of Contents



 

# About Nostradamvs, LLC

We are a NY-based company that provides training and consultation services around cutting-edge technologies including 6G systems, wireless communications, artificial intelligence/machine learning, the internet of things (IoT), distributed ledger technology (DLT), network security, and more.

Our online courses are designed to be intuitive and convenient, allowing you to learn at your own pace and on your own schedule. Whether you are just starting out in the tech industry or are an experienced professional looking to expand your expertise, we have a course that is right for you.

We provide customized in-person and online training for businesses and organizations looking to empower their employees by enhancing their skill sets.
We also provide in-person and online consultation services to businesses looking to optimize their wireless communications & future-proof their ICT systems.

Get in touch today to enhance your professional development and career advancement opportunities; empower your employees; increase your business' productivity and efficiency; and take proactive actions to stay ahead of the curve and anticipate upcoming industry changes.

# Executive Summary

Telecommunications has become an inseparable part of our lives with the advent of the Internet and wireless communications. The number of users and user terminals increased drastically with the widespread use of Internet applications and cellular radio. As a result, transmission frequencies have shifted to higher frequencies in order to meet the increasing demand for higher bandwidths and higher data traffic. Similarly, novel communication techniques are developed to provide reliable communications in fading wireless channels [1].

Increasing transmit power, antenna gains, channel codes, etc., are not enough to meet the requirements of higher data traffic, degradation caused by fading, and increased path losses due to migration to higher frequency bands. Wireless systems, however, can benefit from multiple input multiple output (MIMO) systems, which utilize multiple antennas at the transmitter and/or receiver, in order to overcome these challenges. As part of this paper, we will discuss the benefits of antenna diversity, beamforming, and spatial multiplexing provided by MIMO systems, and their applications in wireless communication [2]-[6]. We will also present a brief discussion of Reconfigurable Intelligent Surfaces (RISs) that are used to direct signals to inaccessible areas to maximize the range, reliability, and efficiency of wireless systems [7], [8].

# 1. Analog beamforming

In free space links, transmitted signals follow straight paths to the receiver. Assuming that a receiver is in the far-field of a transmitter, electromagnetic fields, apart from a term independent of the distance, are characterized by the term exp(-j*kr*)/*r*. As 1/*r* describes the field attenuation of waves with distance *r* from the transmitter, the power of the wave degrades as $1/r^2$ over distance *r*. The term exp(-j*kr*) describes the phase shift, where $k = 2\pi/\lambda$. Thus, the phase of the wave is determined by the electrical distance $r/\lambda$ and the wavelength is found by $\lambda = 0.3/f_{GHz}$ (meters).

In contrast with traditional communication systems that use single transmit and receive antennas, we assume that two antennas transmit to a single receiver located at infinity (see Figure 1). For a fair comparison with single antenna transmission, the transmitter power is equally divided between two antennas. As a result, each signal is multiplied by a normalizing factor of $1/\sqrt{2}$. If path lengths $r_1$ and $r_2$ are equal at the receiver, as in the case for $\theta = 0$, the two received signals add constructively. Consequently, compared with single antenna transmission, the received signal increases by a factor of $\sqrt{2}$; this implies a doubled power. For a receiver located off-boresight, the difference between path lengths $r_1$ and $r_2$ is given by $r_2 - r_1 = dsin\theta$, where *d* denotes the distance between the two transmit antennas. The difference in amplitudes of the two signals is negligible since $1/r_1$ and $1/r_2$ are nearly equal to each other. However, since the received signal components are not in phase, they do not add constructively. The received signal level will therefore be lower compared for the case where $r_1$ and $r_2$ are equal to each other (see Figure 1).

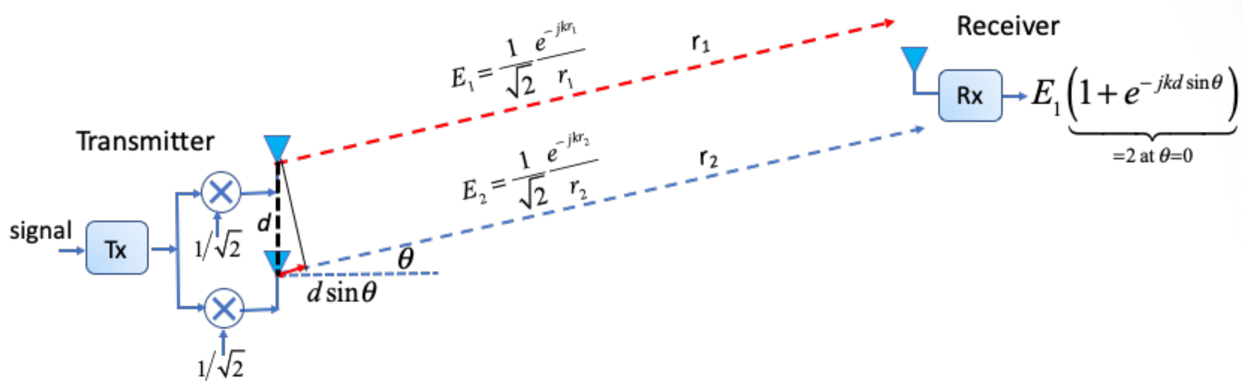


**Figure 1**. Signal transmission by two transmit antennas in off-boresight direction.

Now let us form a beam in the angular direction defined by $\theta=\theta_0$. To this end, we shift the phase of the 2nd transmit antenna compared to the first one by $\exp(jkdsin\theta_0)$, as shown in Figure 2. The phase difference due to the path length difference $r_2$-$r_1$=$dsin\theta$ is then compensated by the phase shift in the 2nd antenna in the direction $\theta=\theta_0$, where the two signals arrive in phase to the receiver. Thus, a beam is formed in the direction $\theta=\theta_0$, where the received signal is maximized, i.e., the received field strength is doubled. However, since the transmit power is equally divided between the two transmit antennas, the received signal strength is actually increased by a factor of $\sqrt{2}$, and the received signal power is doubled compared to single antenna transmission.

Similarly, if we shift the phase of the second transmit antenna compared to the first transmit antenna by $-\exp(jkdsin\theta_0)$. Then, a null is formed in the direction $\theta=\theta_0$ where the received signal vanishes.

 

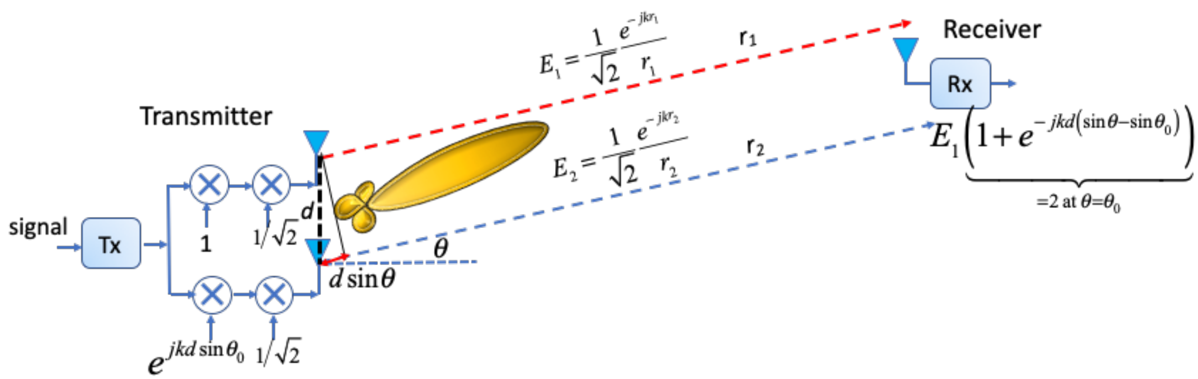


**Figure 2**. Beamforming with two transmit antennas in direction $\theta=\theta_0$.

Now we use an $N$-antenna array for beamforming in the direction defined by $\theta=\theta_0$. Analog phase-shifters are used in the array antennas to control the direction and the radiation pattern of the beam. The phase of $n^{th}$ antenna with normalized transmit power is changed by $\exp(j(n-1)\Psi_0)/\sqrt{N}$, where $\Psi_0 = kdsin\theta_0$. The relative phase shift of the $n^{th}$ path due to path length difference is given by $\exp(-j(n-1)\Psi)$ where $\Psi = kdsin\theta$. The incremental phase shift in the $n^{th}$ path is then given by the sum of the phase shifts due path difference and antenna, $\exp(-j(n-1)(\Psi-\Psi_0))/\sqrt{N}$. The far-field received signal is then multiplied by an array factor, which is given by the sum of incremental phase shifts or a finite Fourier series of incremental phase shifts [2]:

$$|f_a| = \frac{1}{\sqrt{N}}\left|\sum_{n=1}^{N} e^{-j(n-1)(\Psi-\Psi_0)}\right| = \frac{1}{\sqrt{N}}\left|\frac{\sin\left(\frac{N(\Psi-\Psi_0)}{2}\right)}{\sin\left(\frac{\Psi-\Psi_0}{2}\right)}\right| \tag{1}$$

This beam, pointed in the direction $\theta=\theta_0$, behaves as a sin*x*/*x* curve. The maximum value of the array factor, i.e., array gain, is equal to $\sqrt{N}$. This implies an $N$-fold increase in the SNR with respect to single antenna transmission. Null-to-null beamwidth of the beam, given by $2\lambda/(Nd)$, gets narrower as $N$ increases, i.e. it is inversely proportional to the electrical array size. Beamwidth becomes larger if it is directed off boresight. Noting that the array factor is simply given by a finite Fourier series, FIR filters may be used to synthesize beams with desired characteristics, such as beamwidth and sidelobe levels, using different array weights.

Higher array gains due to beamforming enable higher data rates, and improve coverage, by helping users close to the cell edge and providing uniform data rates for all users in the cell. Beamforming can also be used for interference rejection or null management in other directions. Beamforming is widely used in modern radar systems for tracking, jamming and nulling hostile aircraft. Analog beamforming is mandatory for the mmWave frequency range 5G NR.

Note that analog beamforming refers to **single-user** transmission with **one data stream** with an array antenna having a main-lobe, directed to the intended receiver, and some undesired side-lobes. Analog beamforming is mostly associated with **LOS channels**, where path-lengths and the required antenna phase shifts can be determined deterministically.

# 2 Single antenna systems in fading channels

## 2.1 Multipath fading channels

In multipath fading channels, transmitter and receiver do not need to be in LOS of each other, and there may be obstacles around the path. The transmitted signal *s*(*t*) reaches the receiver by following multiple paths due to reflection, diffraction and scattering from obstacles. The description $e^{-jkr}/r$does not apply to multipath channels due to the differences between multipath paths. Instead, the multipath signals are described by random channel gains and phases. The received signal *r*(*t*) in a fading channel with *N* multipaths may be expressed as

$$r(t) = \sum_{n=1}^{N} \alpha_n e^{-j\phi_n} s(t - \tau_n) + w(t) \tag{2}$$

where the $n^{th}$ path is characterized by amplitude $\alpha_n$, phase $\phi_n$, and delay $\tau_n$. If transmitting and/or receiving terminals move fast with respect to each other, then the Doppler frequency shifts should also be considered. Doppler frequency shift due to a terminal moving with velocity *v* is given by

$$f_d = (v/c) f_c \ (\mathrm{Hz}) \tag{3}$$

where *c* denotes the velocity of light, and $f_c$ is the carrier frequency. For long symbol durations, i.e., for sufficiently low data rates, delays may be negligible, and received signal may be written as

$$r(t) \simeq s(t) \sum_{n=1}^{N} \alpha_n e^{-j\phi_n} + w(t) = \alpha e^{-j\phi} s(t) + w(t) \tag{4}$$

When *N* is sufficiently large, the phasor sum of complex channel gains is characterized by $\alpha e^{-j\phi}$. The channel gain $\alpha$ is modeled by Rayleigh distribution, while the channel phase $\alpha$ is uniformly distributed in $[0,2\pi]$. In contrast with the AWGN channel, the amplitude and phase of the received signal in a fading channel also vary randomly due to the term $\alpha e^{-j\phi}$ (see Figure 3).

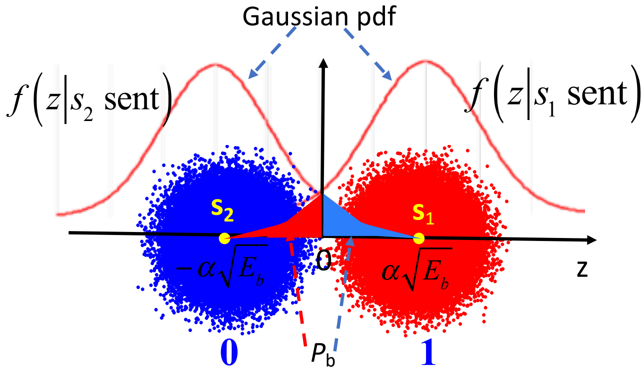


**Figure 3**. The signal constellation for BPSK where the term $\alpha e^{-j\phi}$ is assumed constant. Red and blue clouds show AWGN centered around the symbols $s_1$ and $s_2$.

## 2.2 Bit Error Probability for BPSK in AWGN Channel

In brief, the received signal in an AWGN channel is given by [2]

$$r(t) = s(t) + w(t) \tag{5}$$

which implies that $\alpha = 1$ and $\phi = 0$ in AWGN channels. Assuming that $\alpha$ is a constant, the conditional pdf's, when symbols $s_1$ and $s_2$ are sent, are described by Gaussian pdf's:

$$f\left(z \middle| s_{1,2} \text{ sent}\right) = \frac{1}{\sqrt{\pi N_0}} e^{-\frac{\left(z \mp \alpha\sqrt{E_b}\right)^2}{N_0}} \tag{6}$$

In BPSK, the bit error probability (or equivalently bit error rate, BER) $P_b$ is defined as the probability that a receiver believes $s_1$ ($s_2$) has been sent when in fact $s_2$ ($s_1$) has been sent:

$$\begin{aligned} P_b(\gamma) &= \int_0^\infty f\left(z \middle| s_2 \text{sent}\right) dz = Q\left(\sqrt{2\gamma}\right) \\ \gamma &= \alpha^2 E_b / N_0 \end{aligned} \tag{7}$$

Note that $\alpha \equiv 1$ in AWGN channel. The Gaussian Q-function is defined by:

$$Q(x) = \frac{1}{\sqrt{2\pi}} \int_x^\infty e^{-z^2/2} dz \tag{8}$$

## 2.3 Bit error probability for BPSK in fading channels

The BER in a fading channel is determined by averaging the BER over the random channel gain $\alpha$ or the random SNR $\gamma$:

$$\begin{aligned} \gamma &= \alpha^2 E_b / N_0 \\ \bar{\gamma}_c &= E[\gamma] = E_b / N_0 \end{aligned} \tag{9}$$

The pdf of the SNR in a Nakagami-*m* fading channel is given by

$$f_\gamma(z) = \frac{1}{(m-1)!} \left(\frac{z}{\bar{\gamma}_c / m}\right)^{m-1} \frac{\exp\left(-z / \left(\bar{\gamma}_c / m\right)\right)}{\bar{\gamma}_c / m}, \quad z \geq 0 \tag{10}$$

The pdf for Nakagami-*m* fading is flexible and reduces to the pdf for Rayleigh fading for *m*=1 and to Gaussian pdf as *m* goes to infinity.

Using (10), the BER for BPSK in a Nakagami-m fading channel is [2]:

 

$$P_b = \int_0^{\infty} Q\left(\sqrt{2z}\right) f_\gamma(z)\,dz = \frac{1}{2} - \frac{1}{2}\sqrt{\frac{\bar{\gamma}_c/m}{1+\bar{\gamma}_c/m}} \sum_{n=0}^{m-1} \binom{2n}{n} \frac{1}{\left[4\left(1+\bar{\gamma}_c/m\right)\right]^n} \quad (11)$$

The above expression reduces to the BER for Rayleigh fading channel for $m$=1. Figure 4 shows the BER for BPSK in a Nakagami-$m$ fading channel as a function of $E_b/N_0$ for various values of the fading parameter $m$ [1]. The curve for $m$=1 applies for Rayleigh fading, whereas the curve for $m=\infty$ is for AWGN. The BER in fading is observed to be much worse than in AWGN; the performance difference at BER=$10^{-5}$ is 32.5 dB. Rayleigh fading worsens the BER performance drastically. However, as $m$ increases the channel evolves from Rayleigh fading channel to a Gaussian channel.

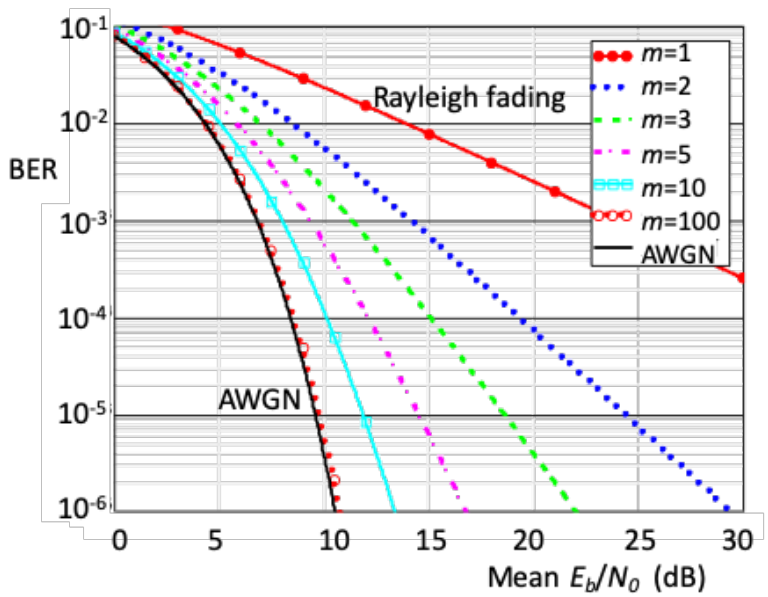


**Figure 4**. Bit error probability for BPSK modulation in a Nakagami-$m$ channel. BER performance due to fading is 32.5 dB worse compared to that for Gaussian channel at BER=$10^{-5}$.

 

# 3. Antenna diversity and beamforming in fading channels

The BER performance in fading channels degrades more than 40 dB at operating BER levels. Using higher transmit powers and/or higher gain antennas are either not practical or not allowed due to health regulations or interference considerations. This problem can be circumvented by diversity, which is based on transmission or reception of the same signal using independent channels in time, frequency, space, or polarization. Thus independently fading multiple copies of the same signal arrive to the receiver. This enables the receiver to make more reliable decision about the transmitted symbol.

Antenna diversity systems are designed for transmission and/or reception of the same signal of a single user by multiple antennas. Antenna diversity is also referred to space diversity. Diversity leads to higher data rates and improved link reliability due to increase in the array gain, which is defined as the output $E_b/N_0$ normalized by mean $E_b/N_0$ of a single channel, and the diversity gain, which mitigates fading and reduces BER for a given output $E_b/N_0$.

The benefit of diversity depends on how the diversity branches are combined. The principal techniques for combining the received diversity branches are

- Selection combining (SC):
  The receiver selects the diversity branch with the highest $E_b/N_0$.
- Equal-gain combining (EGC):
  The receiver estimates the channel phases of diversity branches but not their amplitudes. Then, the signals from received diversity branches are co-phased and summed.
- Maximal ratio combining (MRC):
  The phases and the amplitudes of channel gains of diversity branches are estimated. Then, the diversity branches are weighted by the complex conjugates of their respective channel gains and summed (See Figure 5). This maximizes the output $E_b/N_0$, which is given by sum of the $E_b/N_0$'s of diversity branches.

In this paper, we will discuss only MRC receiver diversity, where a signal transmitted from a single transmit antenna arrives at multiple receive antennas that are separated by more than half wavelength in order to ensure independent fading between the antennas (see Figure 5). The received signal may then be written, in terms of the complex channel gains, as [2]:

$$r(t)=\left(\left|h_{11}\right|^2+\left|h_{21}\right|^2+\cdots+\left|h_{N_R 1}\right|^2\right)s(t)+\left(w_1 h_{11}^*+w_2 h_{21}^*+\cdots+w_{N_R} h_{N_R 1}^*\right) \tag{12}$$

where $w_i$ denotes the AWGN at $i^{th}$ diversity branch. The output $E_b/N_0$ is given by the sum of $E_b/N_0$'s of $N_R$ diversity branches:

$$\gamma=\left(\alpha_{11}{}^2+\alpha_{21}{}^2+\cdots+\alpha_{N_R 1}{}^2\right)E_b/N_0 \tag{13}$$

 

$$E[\gamma] = \bar{\gamma} = N_R \bar{\gamma}_c, \quad \bar{\gamma}_c = E_b/N_0 \tag{14}$$

The pdf of the output $E_b/N_0$ in a Rayleigh fading channel, when $N$ diversity branches with identical mean $E_b/N_0$'s are maximal-ratio combined, is given by

$$f_N(\gamma) = \frac{\gamma^{N-1}}{(N-1)!} \frac{e^{-\gamma/\bar{\gamma}_c}}{\bar{\gamma}_c} \tag{15}$$

Note that the above pdf reduces to the well-known Rayleigh pdf for $N$=1.

MRC is the best performing combining technique since the output SNR is increased by a factor of $N_R$. MRC combining may also be interpreted as digital beamforming. A receiver estimates periodically the channel gain in each diversity branch based on the training sequences transmitted by the transmitter. CSI, which is updated as channel gains vary significantly, is used for co-phasing and combining diversity branch signals. Note that accurate estimation and frequent update of the CSI may be challenging and costly.

The BER for BPSK modulation for MRC is determined by averaging the BER with random SNR, $\gamma$:

$$P_b = \int_0^\infty Q\left(\sqrt{2\gamma}\right) f_N(\gamma)\, d\gamma \tag{16}$$

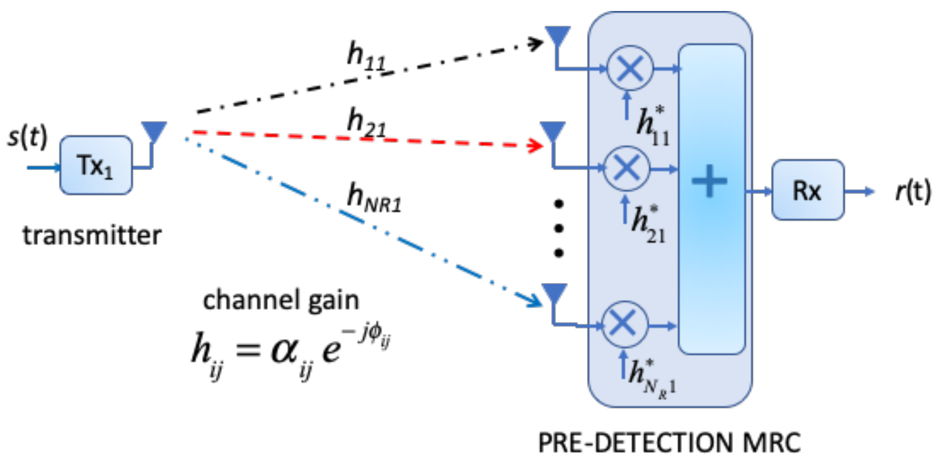


**Figure 5**. Maximal ratio combining (MRC)

The result is given by [2]

$$P_b = \frac{1}{2} - \frac{1}{2}\sqrt{\frac{E_b/N_0}{1+E_b/N_0}} \sum_{n=0}^{N-1} \binom{2n}{n} \frac{1}{\left[4\left(1+E_b/N_0\right)\right]^n} \tag{17}$$

Note that (17) is a special case of (11) for $m$=1. Figure 6 shows the BER for BPSK modulation vs branch $E_b/N_0$ expressed in dB for various values of $N$, the number of branches for a MRC system

 

[2]. There is a rapid decrease in BER with an increase in the number of diversity branches, *N*, and this decrease slows down as N exceeds five. For *N* exceeding five, the MRC system in a Rayleigh fading channel outperforms the corresponding BER in AWGN channel. For *N*=5, the BER performance is improved by more than 30 dB due to MRC diversity combining. One may thus conclude that MRC diversity mitigates Rayleigh fading effects, and provides a unique opportunity to communicate more reliably and at higher data rates.

Maximal ratio transmission (MRT) refers to transmit antenna diversity (see Figure 7). The receiver estimates channel gains of each diversity branch, and feeds them back to the respective transmit antennas. The transmitter weighs the signal of each branch with respective estimated normalized channel gains before transmission.

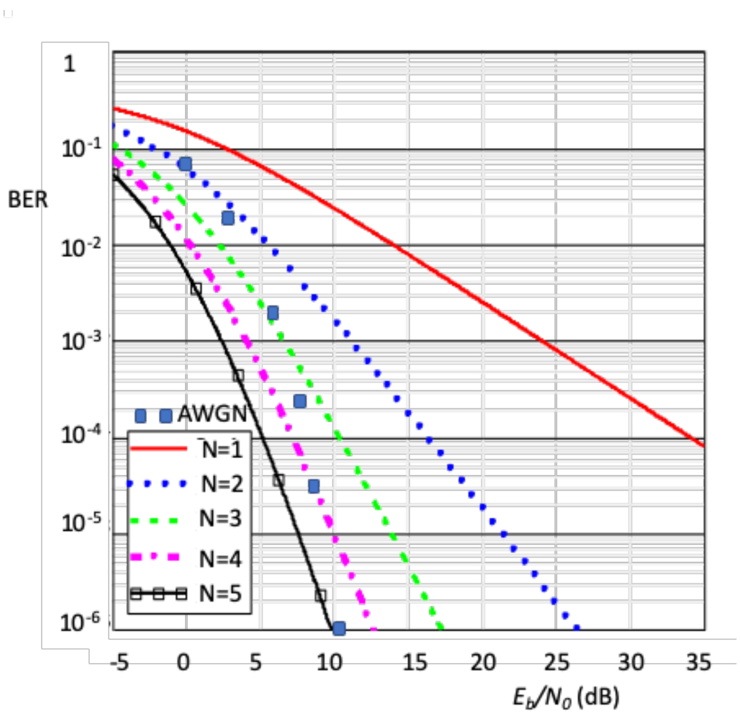


**Figure 6**. Bit error probability for BPSK for MRC in a Rayleigh fading channel vs branch $E_b/N_0$.

From Figure 7, the received signal *r*(*t*) may be written as [2]

$$r(t) = \frac{1}{\|\mathbf{h}\|}\left(|h_{11}|^2 + |h_{12}|^2 + \cdots + |h_{1N_T}|^2\right)s(t) + w(t) \tag{18}$$

where transmit powers of each of the $N_T$ antennas are normalized by

$$\|\mathbf{h}\| = \left(|h_{11}|^2 + |h_{12}|^2 + \cdots + |h_{1N_T}|^2\right)^{1/2} \tag{19}$$

The $E_b/N_0$ at the receiver output is determined from the last two equations as follows:

$$\gamma = \left(\alpha_{11}{}^2 + \alpha_{12}{}^2 + \cdots + \alpha_{1N_T}{}^2\right) E_b / N_0$$

$$E\left[\gamma\right] = \bar{\gamma} = N_T \bar{\gamma}_c, \quad \bar{\gamma}_c = E_b / N_0 \tag{20}$$

The SNR $\gamma$ of the receiver output is equal to the sum of $E_b/N_0$'s of $N_T$ diversity branches. The array gain is maximized and is equal to the number of diversity branches $N_T$. Hence, array and diversity gains for MRC and MRT are identical. Therefore, Figure 6 is also applicable for MRT. Note that MRT may be used for digital beamforming in both LOS and NLOS links.

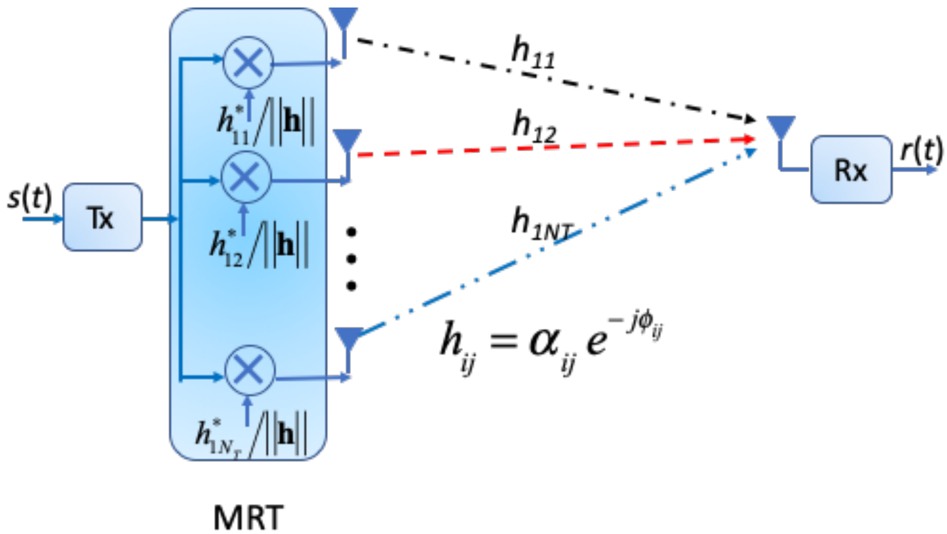


**Figure 7**. Maximal ratio transmission (MRT)

 

# 4. MIMO Systems

In antenna diversity systems, we considered the following cases:

- MRT: Multiple antennas are used by one user to transmit data to a single receiver antenna used by another user, and
- MRC: A single antenna is used by one user to transmit data to a multiple-antenna receiver for another user.

Furthermore, these systems can also be used for analog beamforming by shifting the antenna phases.

MIMO stands for multiple-input multiple-output. MIMO systems are capable of transmitting multiple data streams to multiple receivers, each of which has multiple antennae. Therefore, a MIMO system is simply a generalization of the above-considered transmit and receive antenna systems. In that sense, a MIMO system with a single receive (transmit) antenna reduces to MRT (MRC). In a similar manner, a MIMO system with a single transmit and receive antenna reduces to a single antenna system.

A MIMO system has more antennas than transceivers, which implies that a transceiver may employ multiple antennas for improved performance. This is a cost-effective approach since antennas are in general cheaper than transceivers.

Figure 8 shows the block diagram of a MIMO system with $N_T$ transmit and $N_R$ receive antennas.

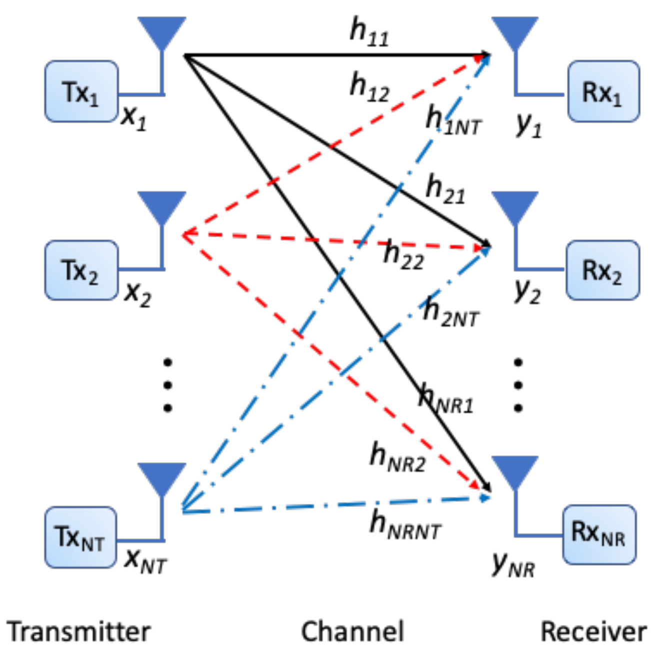


**Figure 8**. Block diagram of a MIMO system with $N_T$ transmit and $N_R$ receive antennas

 

Such a system is described by a channel matrix $H$ with $N_T$ columns and $N_R$ rows:

$$H = \begin{pmatrix} h_{11} & h_{12} & \cdots & h_{1N_T} \\ h_{21} & h_{22} & \cdots & h_{2N_T} \\ \vdots & \vdots & \ddots & \vdots \\ h_{N_R1} & h_{N_R2} & \cdots & h_{N_RN_T} \end{pmatrix} \tag{21}$$

A MIMO system has an order of diversity equal to the product of the number of transmit and receive antennas, $N_RN_T$, as all receive and transmit antennas communicate with one another and channel gains fade independently. This evidently leads to high array and diversity gains, i.e. high output SNR and low BER. As we will discuss below, MIMO systems not only provide greater antenna diversity, but also spatial multiplexing and beamforming capabilities. Therefore, they enable higher throughput and capacity, lower BERs, and increased SINR. MIMO systems may also be used to provide resilience against interference and jamming.

The following factors are involved in the design and performance of MIMO systems:

- Propagation over multiple paths, which has a significant impact on the BER
- Data transmission strategies to make best use of MIMO systems to maximize capacity and throughput
- Coupling between antenna elements, that affects the diversity order and the output SINR.

The channel matrix elements are uncorrelated if the spacing between adjacent antennas exceeds half the wavelength. For example, at 2.4 GHz, the half wavelength is 6.25 cm. MIMO elements can be spaced closer together at higher frequency bands than at 2.4 GHz. Due to this, a MIMO antenna system with half wavelength antenna spacings can be easily packed into a small space. If the antenna elements are closer than half wavelength, then the correlation between them reduces the MIMO system performance. Here we assume that channel matrix elements are uncorrelated.

MIMO systems operate in

- Urban environments, where diversity, beamforming, and spatial multiplexing can be used to meet high data rate requirements in small cells
- Rural environments to compensate large path losses, and to provide uniform data rates over large cells
- Outdoor-to-indoor coupling for fixed wireless access scenarios
- Indoor environments for Wi-Fi access

The block diagram of a $N \times N$ MIMO-MRC system is shown in Figure 9. Input-output relationship in a MIMO-MRC system is given by

$$\begin{pmatrix} r_1 \\ r_2 \\ \vdots \\ r_N \end{pmatrix} = H^H H \begin{pmatrix} x_1 \\ x_2 \\ \vdots \\ x_N \end{pmatrix} + H^H \begin{pmatrix} w_1 \\ w_2 \\ \vdots \\ w_N \end{pmatrix} \tag{22}$$

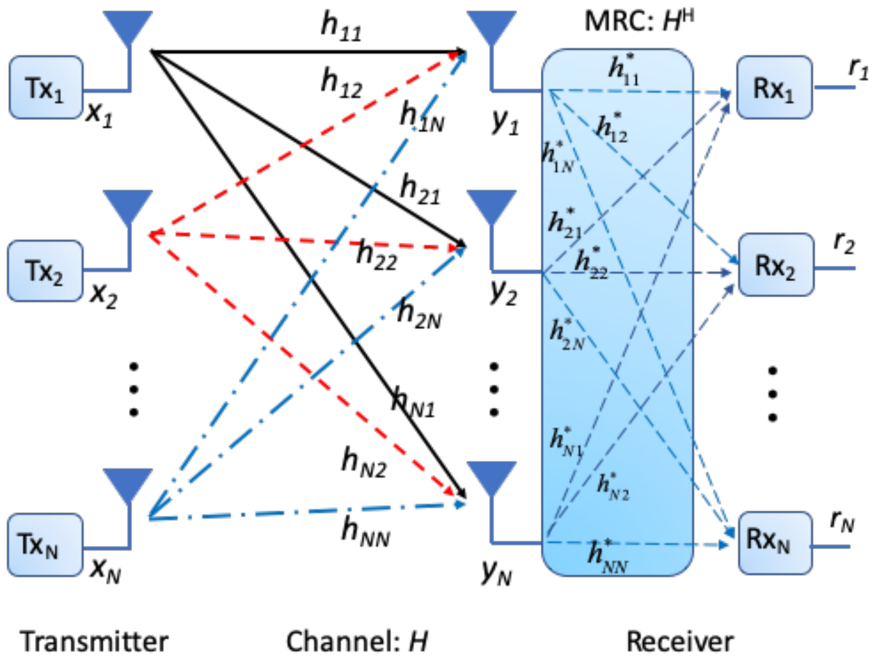


**Figure 9**. Block diagram of a $N \times N$ MIMO-MRC system

In a MIMO-MRC system, the complex channel gains, i.e. CSI, are estimated by the receiver. This brings considerable overhead to the MIMO-MRC system because of the resources allocated for accurate estimation of the CSI and performance degradation due to inaccuracies in the CSI.

The block diagram of a $N \times N$ MIMO-MRT system is shown in Figure 10.

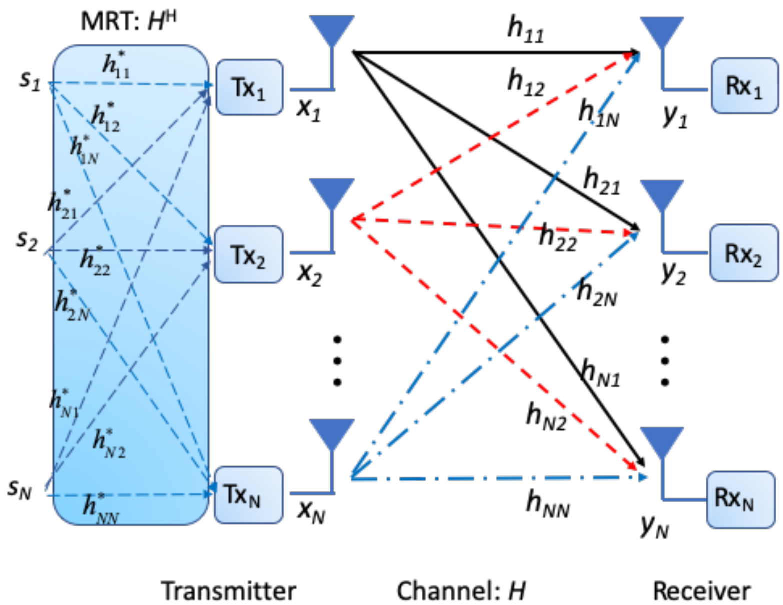


**Figure 10**. Block diagram of a *N*×*N* MIMO-MRT system

The input-output relationship in a MIMO-MRT system is given by

$$\begin{pmatrix} y_1 \\ y_2 \\ \vdots \\ y_N \end{pmatrix} = HH^H \begin{pmatrix} s_1 \\ s_2 \\ \vdots \\ s_N \end{pmatrix} + \begin{pmatrix} w_1 \\ w_2 \\ \vdots \\ w_N \end{pmatrix} \tag{23}$$

In a MIMO-MRT system the complex channel gains estimated by the receiver are fed-back to the transmitter that pre-codes the signals to be transmitted. This brings considerable overhead to the MIMO-MRT system since it requires a feed-back channel for CSI and causes degradation in system performance due to inaccuracies in the CSI.

The random matrices $HH^H$ and $H^H H$ are described by Wishart distribution [2]. Here $(.)^H$ shows the Hermitian, i.e. conjugate transpose, of a matrix. If $N_R$ and $N_T$ are not equal, then the Wishart matrix has $n$=min($N_R$,$N_T$) non-zero eigenvalues. The rest $|N_R - N_T|$ of the eigenvalues are identically equal to zero. The maximum eigenvalue of the Wishart matrix determines the MIMO system's performance. The Wishart matrices $H^H H$ and $HH^H$ have identical eigenvalues, and account for MIMO-MRC and MIMO-MRT, respectively. Hence, MIMO-MRC and MIMO-MRT have identical performances. Also note that $N_T \times N_R$ and $N_R \times N_T$ MIMO systems have identical performances. Similarly, 1 × 1 MIMO system implies single transmitter and single receiver and its eigenvalue is described by Rayleigh pdf. The eigenvalue denotes SINR since MIMO systems take multi-user interference into account. While MRC and MRT are special cases of MIMO systems, they ignore multi-user interference and only consider the signal-to-noise ratio. Therefore, MRC and MRT systems perform better than the corresponding MIMO systems. For example, a $N_T \times N_R$ MIMO system performs slightly worse than $1\times N_T N_R$ (MRC) or $N_T N_R \times 1$ (MRT) systems.

For small values of $n$=min($N_R$,$N_T$), analytical expressions for the pdf's of the maximum eigenvalue are available and are given below [2, (13.17)-(13.22)]:

$n$=1, $m$≥1:

$$f(\lambda)=\frac{1}{(m-1)!}\lambda^{m-1}\,e^{-\lambda} \tag{24}$$

$n$=$m$=2:

$$f(\lambda)=e^{-\lambda}\left(\lambda^{2}-2\lambda+2\right)-2e^{-2\lambda} \tag{25}$$

$n$=2, $m$=3:

$$f(\lambda)=e^{-\lambda}\left(3\lambda-2\lambda^{2}+\lambda^{3}/2\right)-e^{-2\lambda}\left(3\lambda+\lambda^{2}\right) \tag{26}$$

$n$=$m$=3

$$\begin{aligned} f(\lambda)=&\frac{1}{4}e^{-\lambda}\left(12-24\lambda+24\lambda^{2}-8\lambda^{3}+\lambda^{4}\right)\\ &-\frac{1}{2}e^{-2\lambda}\left(12-12\lambda+6\lambda^{2}+2\lambda^{3}+\lambda^{4}\right)+3e^{-3\lambda}\end{aligned} \tag{27}$$

In order to determine how MIMO size affects BER performance for BPSK modulation, $f_N(\gamma)$ in (16) may be replaced by the pdf's of the highest eigenvalues listed in (24)-(27). Figure 11 shows the BER for BPSK modulation as a function of $E_b/N_0$ for various MIMO sizes [2]. The increase in MIMO size results in dramatic improvements in BER performance for small MIMO sizes. For MIMO sizes exceeding 3×3, the BER performance is better than in AWGN channels, as was also observed in MRT and MRC. As MIMO size increases, however, BER performance improvement slows down because the diversity benefits diminish as the number of diversity branches, $N_T N_R$, exceeds ten. An additional problem with large MIMO diversity systems may be the increased overhead associated with channel estimation, i.e., CSI.

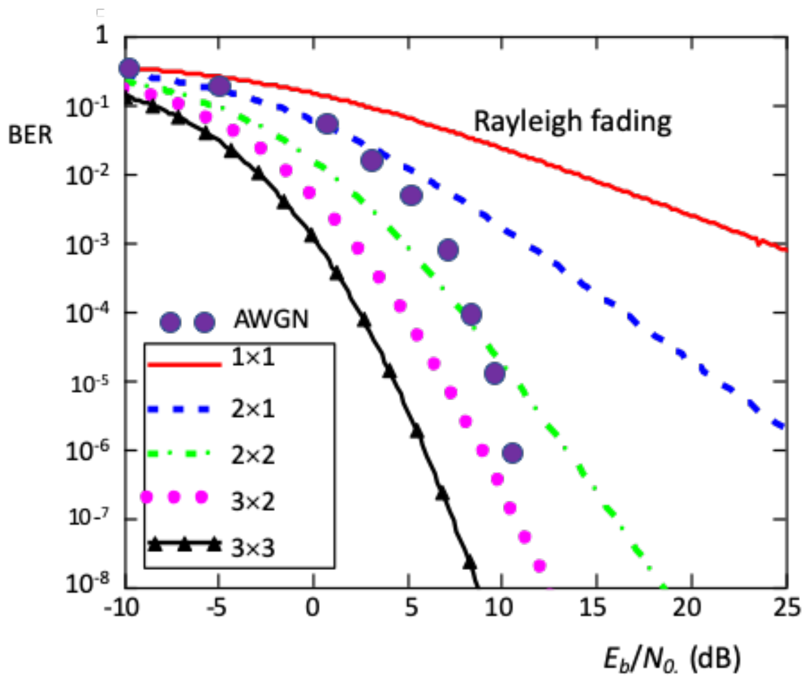


**Figure 11.** BER for BPSK modulation as a function of $E_b/N_0$ for various MIMO sizes

The mean values of MIMO systems' eigenvalues denote the mean SINRs. Table 1 compares them with the array gains of the corresponding MRC/MRT systems. To ensure a fair comparison, both systems are compared using the same number of diversity branches. The array gain of MRC systems is equal to the number of receiving antennas and is higher than that of equivalent MIMO systems, since MIMO systems consider multi-user interference, while MRC systems do not. As MIMO size increases, the MRC array gain advantage becomes more significant due to the fact that multi-user interference is greater for larger MIMO arrays. The resource requirements and effects of imperfect CSI estimation may, however, be comparable in both cases.

## 4.1 Massive MIMO

The term massive MIMO refers to a MIMO system consisting of many smart antennas, i.e. antennas with embedded radio transceivers that are managed appropriately. It is more advantageous to use massive MIMO in the mmW band due to the fact that hundreds of antennas can be packed into a small space. In the mmW band (30-300 GHz), wavelengths are shorter than one centimeter, so a 100×100 MIMO system can be packet into an area 0.5m × 0.5m with half wavelength antenna spacing. MIMO size decreases at frequencies higher than 30 GHz.

**Table 1**. Comparison of the array gain of MRC/MRT systems with the largest eigenvalue of the corresponding MIMO systems [2, Table 13.1].

| MIMO | | MRC | | Comparison |
|---|---|---|---|---|
| Size | Max. eigenvalue | Size | Array gain | MRC array gain advantage (dB) |
| 1 × 1 | 1 | 1 × 1 | 1 | 0 |
| 1 × 2 | 2 | 1 × 2 | 2 | 0 |
| 2 × 2 | 3.5 | 1 × 4 | 4 | 0.58 |
| 2 × 3 | 4.88 | 1 × 6 | 6 | 0.90 |
| 2 × 4 | 6.19 | 1 × 8 | 8 | 1.11 |
| 3 × 3 | 6.52 | 1 × 9 | 9 | 1.40 |
| 4 × 4 | 9.77 | 1 × 16 | 16 | 2.15 |

In the mm-wave band, waves cannot penetrate walls and other obstacles. The surfaces with millimeter-scale roughness behave differently from flat surfaces. This results in diffuse scattering, which in turn affects the strength and polarization of the received signal. Therefore, channel modeling in the mm-wave band should account for the effects of diffuse scattering. As a result of the high density of obstacles and walls in indoor environments, beamforming in the mm-wave band presents a challenging problem. On the other hand, received signals in outdoor links in the mm-wave band suffer high atmospheric and precipitation losses.

MIMO systems in the mm-wave band are still capable of achieving very high antenna gains, even though they are small and can be integrated into boards and chip circuits. CMOS production technologies offer substantial reductions in cost and size. In addition, power-efficient circuits, smart antennas, and mm-wave band devices enable the use of wider bandwidths available for wireless communications in the mm-wave band. Because mm-wave signals cannot penetrate walls and other obstacles, frequency reuse distances are shorter in the mm-wave band. Due to the high data rates, it is possible that the channel will experience frequency-selective fading, resulting in a more complex receiver design, but with additional diversity benefits.

## 4.2 Single-user MIMO vs multi-user MIMO

In a single-user MIMO (SU-MIMO), data streams are transmitted to a single user in a specified time/frequency grid using all antennas. Thus, a SU-MIMO user can potentially transmit at higher data rates by utilizing the entire bandwidth combined with high array and diversity gains. Therefore, shorter transmission periods are usually sufficient for SU-MIMO users.

It has been discussed above that MRC/MRT diversity systems that have more than five antennas and MIMO systems with more than three antennas outperform AWGN systems. As the number of antennas increases, fading mitigation gains are reduced. In this regard, it may not be cost-effective to allocate all antennas in massive MIMO systems to a single user. Instead, it may be more economical to utilize massive MIMO capacity by simultaneously serving multiple users at both ends. In this respect, massive MIMO provides an excellent opportunity to spatially multiplex signals for multiple users, referred to as multi-user MIMO (MU-MIMO).

As shown in Figure 12, SU-MIMO users can transmit data in time-division multiplexing by using the full bandwidth, all antennas and total transmit power. However, MU-MIMO users communicate by exploiting non-overlapping chunks of time-bandwidth, i.e., time-and frequency division multiplexing, and sharing the transmit power and antennas.

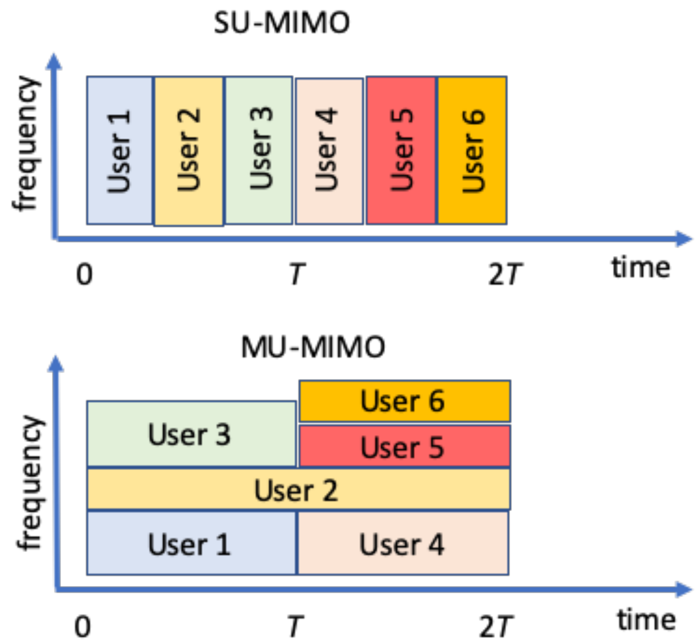


**Figure 12.** A depiction of the time-frequency usage in SU-MIMO and MU-MIMO.

MU-MIMO wireless systems enable simultaneous transmission of multiple spatial streams by allocating different sub-bands and transmit power levels to different users (see Figure 13). Thus, available bandwidth can be utilized in a flexible and economical manner, and users will be able to access the system more quickly.

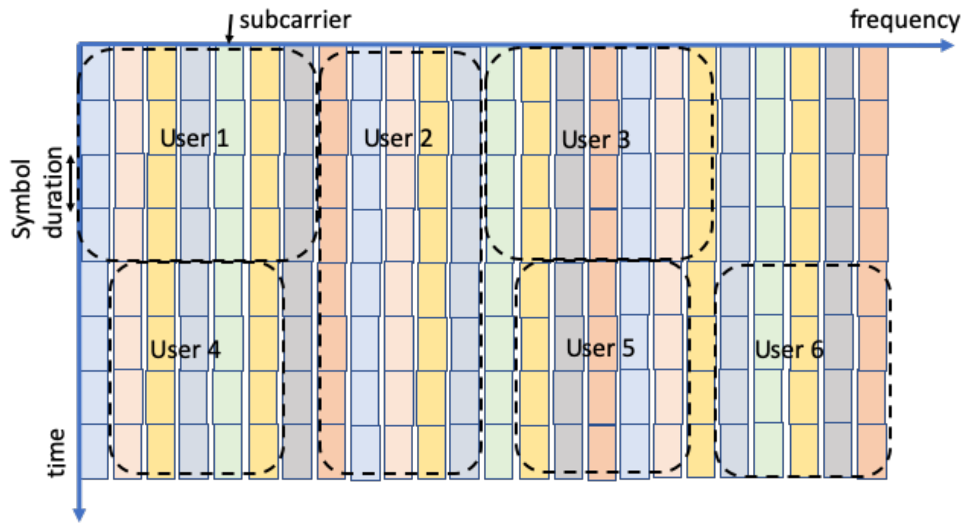


**Figure 13.** Non-overlapping time-frequency chunks allocated to users in multiple spatial streams

Orthogonal Frequency Division Multiplexing (OFDM) is a wideband transmission technique suitable for MU-MIMO [2]. An OFDM system consists of a large number of orthogonal narrow-band subcarriers with relatively long symbol durations, thereby ensuring flat fading. In orthogonal frequency division multiple access (OFDMA), users are allocated non-overlapping time-frequency chunks in multiple spatial streams (See Figure 13). This increases the efficiency and reliability of transmissions as well as the number of users that can be supported by a BS. Thus, MU-MIMO systems provide space, time, and frequency diversity.

Now let us consider a 10×10 MU-MIMO system with three users. A 4x4 MIMO system is used by users 1 and 3, while a 2x2 MIMO system is used by user 2 (see Figures 14 and 15). The three users transmit simultaneously. The receivers combine the signals at their respective MIMO antenna terminals. OFDM can be employed to achieve frequency multiplexing. These three streams are orthogonal in frequency as non-overlapping orthogonal frequency sub-bands are allocated to these users. The total transmit power is allocated among three users based on range, the number of MIMO antennas, the number of subcarriers, and the data rate. In both NLOS and LOS scenarios, channel gains and transmit powers can be designed to achieve higher capacities through spatial multiplexing.

Similarly, the MIMO multiple-access-channel, MIMO-MAC, represents a MIMO uplink where multiple users transmit to a single receiver wireless network.

MU-MIMO can meet the following demands and user preferences:

- Significant increases in the number of Wi-Fi and cellular network users and devices, especially in urban areas, and hot spots.
- Ever increasing demands for increased throughput and capacity, e.g. streaming music and video as well as video conferencing.
- User preferences for using a single and simpler device for many applications.
- Demands in enterprise networks for new applications to increase employee mobility.

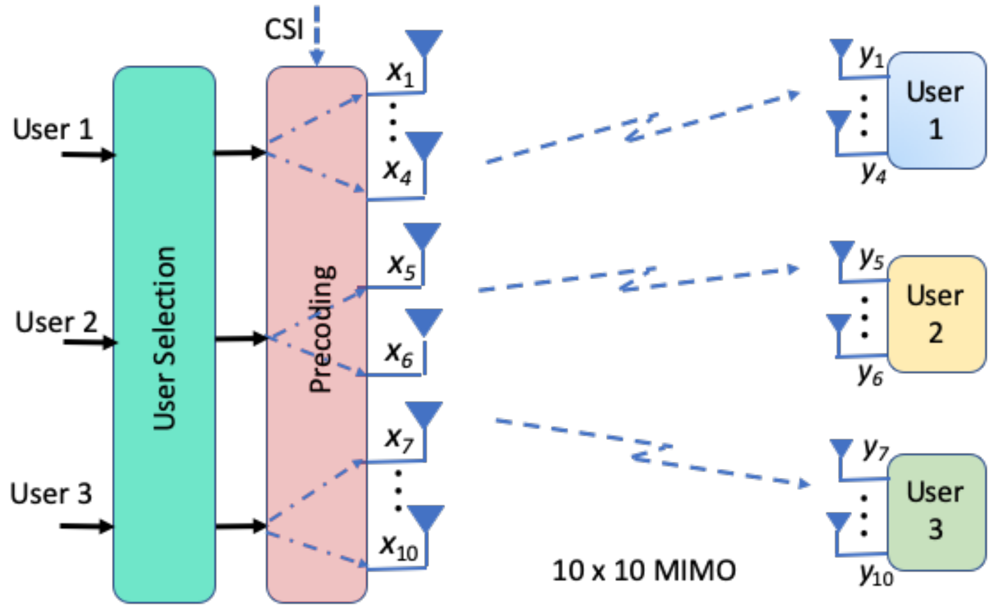


**Figure 14.** A 10×10 MU-MIMO downlink system transmitting to three receivers. User 1 uses 4×4 MIMO, user 2 uses 2×2 MIMO, and user 3 uses 4×4 MIMO.

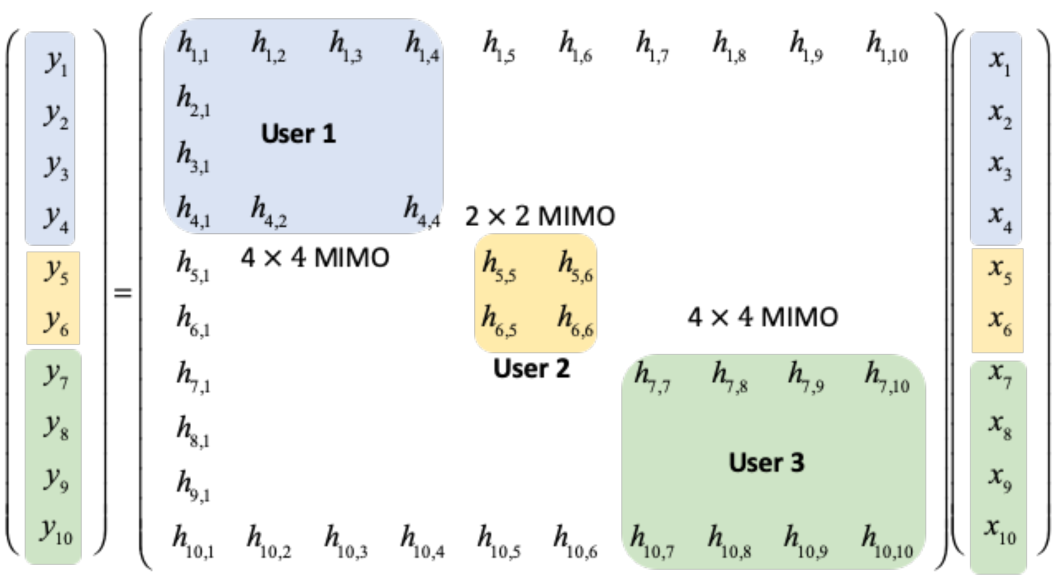


**Figure 15**. Channel matrix for the MIMO downlink system considered in Figure 14, i.e., for a 10×10 MIMO system with three users employing 4×4, 2×2 and 4×4 MIMO antennas.

## 4.3 Digital beamforming

In analog beamforming, a single user transmits a single data stream using multiple antennas, full bandwidth and total transmit power. The use of phase shifters at transmit antennas ensures constructive interference between copies of the same signal at the receiver.

A digital beamformer, also known as a precoder, is a generalization of an analog beamformer. In contrast to analog beamforming, digital beamforming is based on phase changes in signals rather than antennas. The transmitted signals are matched to the channel gains in such a way that the multipath components add constructively at the receivers. Digital beamforming may also be used for interference cancellation. It is also possible to use massive MIMO systems to spatially multiplex multiple data streams to users on multiple beams with higher array gains.

For example, consider a MIMO beamforming system depicted in Figure 16. A signal *s*(*t*) is transmitted using $N_T$ transmit antennas after being weighted by a transmit weighting factor $\mathbf{w}_t$. Similarly, signal components received by $N_R$ receive antennas are weighted by a receive weighting factor $\mathbf{w}_r$ and are added. The output SNR is given by [2,13.86]

$$\gamma = \bar{\gamma}_c \, \lambda_{\max}, \quad \bar{\gamma}_c = E_b / N_0 \qquad (28)$$

where $E_b/N_0$ denotes the branch SNR, and $\lambda_{max}$ represents the pdf of the maximum eigenvalue corresponding to $N_T \times N_R$ MIMO system. The mean value of the maximum eigenvalue is compared in Table 1 with the array gain of the corresponding MRC/MRT system.

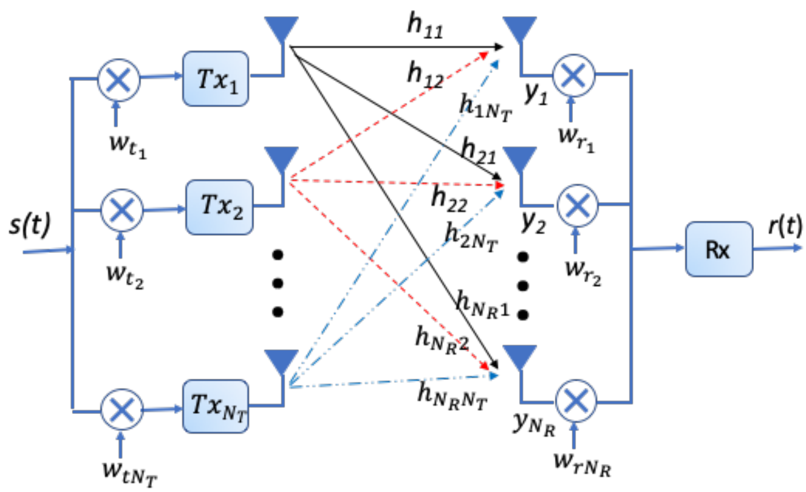


**Figure 16**. MIMO beamforming.

Switched beamforming refers to the formation of multiple beams covering all directions, and one or more beams can be switched on when needed. Adaptive beamforming is more suitable than switched beamforming because of its ability to eliminate interference and reduce power consumption. In optimal beamforming, analog and digital beamforming are combined with optimal algorithms. Digital beamforming is used in LTE Advanced Pro and in 5G NR for MU-MIMO users. 5G base stations may use analog, digital and hybrid beamforming. For example, inside an analog beam, digital beamforming may be used for MU-MIMO or SU-MIMO users.

For example, Figure 17 shows that spatial multiplexing (digital beamforming) may be used to transmit to two users over a single analog beam. The optimal algorithms are used to estimate the direction of arrival of user signals in azimuth and elevation and to carry out appropriate signal processing required for beamforming. Finite impulse response filters may be used to implement optimal beamforming. Optimal beamforming in massive MIMO systems meets the requirements of next-generation wireless communication systems. The field of narrowband and wideband digital beamforming has received considerable research attention in recent years. Wideband beamforming is more challenging in massive MIMO systems operating in mm-wave bands than in lower frequency bands.

Beamforming maximizes the array gain, i.e., mean value of the maximum eigenvalue, as well as the diversity gain, i.e., lower BERs. The use of beamforming has many advantages for mobile operators, users, and the environment. Moreover, it enhances network capacity, coverage, energy and spectral efficiency, as well as the user experience. Beamforming enables dynamic cell coverage to meet the needs of fast-moving users, and those in areas where network coverage is not satisfactory. Beamforming also ensures uniform data speeds and latency across the cells, especially in densely populated areas. As a result, higher order modulations can be used to provide higher data rates to distant users. As a result of the extended coverage, the BS density decreases. It is also possible to use MIMO beamforming for indoor Wi-Fi systems and for coupling from outdoor to indoor environments. Beamforming with narrow beams can provide better protection against interception, interference and jamming. Beamforming with MU-MIMO can maximize transmission in the desired direction while simultaneously eliminating undesired users [1], [2], [6]. In the mm-wave band, shorter ranges, and relatively narrow beamwidths also provide significant improvements in security and privacy [7].

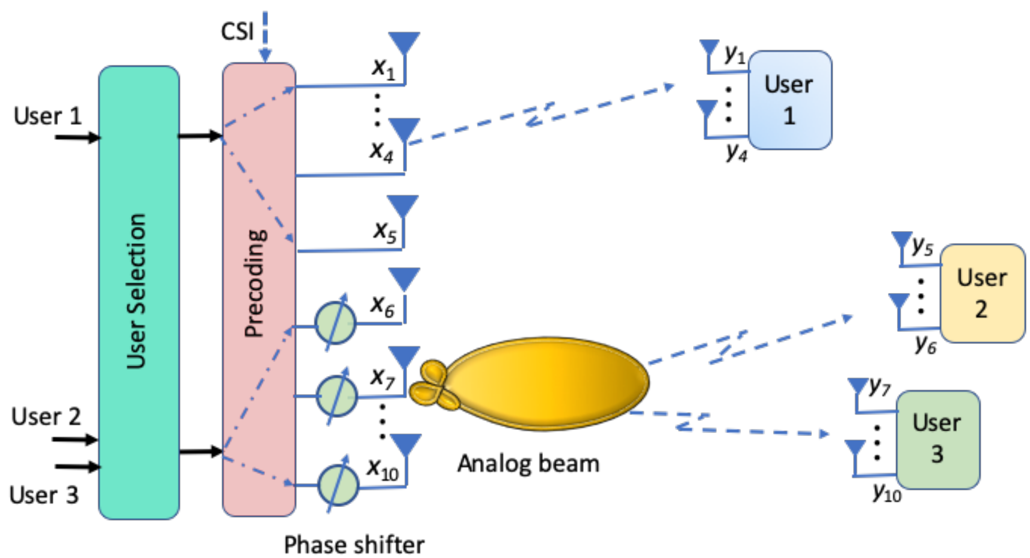


**Figure 17.** Hybrid beamforming

# 5. Reconfigurable Intelligent Surfaces

Traditional wireless systems regard the radio channel as an uncontrollable entity that scatters propagating signals randomly as a wide range of surfaces along the propagation path. This results in random constructive and destructive interferences of the received signal components, i.e., fading. In the same way that MIMO systems enhance wireless systems' performance, Reconfigurable Intelligent Surfaces (RISs) direct signals to inaccessible areas to maximize the range, reliability, and efficiency of wireless systems. RIS is a programmable surface structure that controls the reflection of electromagnetic (EM) waves by altering its electric and magnetic properties [8], [9]. To improve the link quality, RISs between transmitters and receivers can be strategically positioned to direct signals towards the receiver.

Metasurfaces and conventional antenna arrays are two main approaches to implementing an RIS to control signal characteristics (e.g., reflection, refraction, absorption, focusing, and polarization). Metasurfaces consist of two-dimensional arrays of structural elements which are electrically thin and dense. Their constitutive elements provide them with desired properties. Known as meta-cells, these elements have a much smaller size than the wavelength of the signal. In addition to controlling electromagnetic propagation, metasurfaces can be used to realize complex operations such as data modulation, signal processing, and storage of EM pulses for short periods. Another simple implementation of RIS involves electrically tunable reflecting antenna arrays that dynamically adjust radiation patterns. Specifically, a large number of low-cost and passive antenna elements in RIS operate as reflectors with no need for RF chains as in conventional MIMO systems. The most common RIS structures are placed on a wall to direct BS signals in the desired direction. However, metasurface-based RIS may also cover all surfaces (walls, furniture, clothes, etc.).

RISs would first absorb a signal directed at it. This signal would be processed by a microcontroller and then regenerated and transmitted in a specific direction by antenna arrays and metasurfaces. In this manner, they can be used to improve the availability of cellular and global navigation satellite system (GNSS) signals in areas where they are not naturally accessible. It is also possible to use deflection of signals to reduce the path taken by signals to reach the receiver. This improves the network's efficiency.

RIS applications are expected to increase as the 5G and 6G frequency bands migrate into the mmWave and THz regions. The reason for this is that signals in these frequency bands attenuate rapidly and cannot penetrate walls in the same way as sub-6 GHz signals used by cellular technologies. RISs may also be used to redirect such high-frequency signals to reach indoor users, and, in addition, to remodulate them according to a specific mid-propagation algorithms.

# 6. Conclusions

Internet applications and cellular radio systems play an important role in our daily lives. The increasing number of users and terminals, the demand for higher data traffic, and the need for improved services have created a need for novel and reliable communication techniques. It is difficult to address these issues with traditional measures, such as increasing transmit power or antenna gains, utilizing channel codes, etc., particularly in fading channels. The MIMO systems provide a great opportunity to provide cost-effective solutions to these issues, and to meet requirements for power- and spectrum-efficient communications. Operation in mmW band greatly facilitates the use of massive MIMO systems, which embody diversity, beamforming, and spatial multiplexing as special cases.

The MIMO systems, coupled with OFDM, can provide

- Antenna, frequency and time diversity
- Single- and multi-user communications
- Spatial multiplexing
- Analog and digital beamforming to improve receiver SNR and balanced coverage in cellular systems
- Economic and optimized use of the transmission bandwidth, transmit power and transmit/receive antennas
- Improve system reliability, throughput, capacity as well as services
- Opportunity to relieve Wi-Fi systems from demands for increased traffic

# References


[1] I. F. Akyildiz, A. Kak, and S. Nie, 6G and Beyond: The Future of Wireless Communications Systems, IEEE Access, vol.8, pp.133995-134030, 2020.

[2] Mehmet Şafak, Digital Communications, J. Wiley & Sons: Chichester, UK, 2017.

[3] K. Hosseini, W. Yu, and R. S. Adve, Large-scale MIMO versus network MIMO for multicell interference mitigation, IEEE J. Sel. Topics Signal Process., vol. 8, no. 5, pp. 930 941, Oct. 2014.

[4] Emil Björnson, et al., 25 Years of Signal Processing Advances for Multiantenna Communications, arXiv:2304.02677v1 [eess.SP] 5 Apr 2023.

[5] E. Björnson et al., Massive MIMO is a reality What is next? Five promising research directions for antenna arrays, 2019, arXiv:1902.07678.

[6] E. Ali, M. Ismail, R. Nordin, and N.F. Abdulah, Beamforming techniques in massive MIMO systems in 5G: overview, classification, and trends for future research, Frontiers of Information Technology & Electronic Engineering, vol.18, no.6, pp.753-772, 2017

[7] P. Porambage et al., 6G Security Challenges and Potential Solutions, 2021 Joint European Conference on Networks and Communications (EuCNC) & 6G.

[8] E. Björnson, and L. Sanguinetti, Power scaling laws and near-field behaviors of massive MIMO and Intelligent reflecting surfaces, IEEE Open Journal of the Communications Society, vol.1, pp.1306-1324, 2020.

[9] H. Abumarshoud et al., LIFI through reconfigurable intelligent surfaces, IEEE Vehicular Technology Magazine, pp.37-46, March 2022.

# Contact

Contact us for inquiries


Nostradamvs LLC, 418 Broadway, STE N, Albany, NY, 12207

info@nostradamvsllc.com

www.nostradamvsllc.com